Drive-induced damping due to the equilibrium fluctuations of a thermal bath

Arnab Chakrabarti* and Rangeet Bhattacharyya†
Department of Physical Sciences
Indian Institute of Science Education and Research Kolkata
Mohanpur – 741246, West Bengal, India

Quantum master equations usually describe the linear response of a driven dissipative system to an external drive. The Rabi oscillations and the relaxation from system-bath coupling, as predicted by these equations, forms the basis of all resonant spectroscopy and applications of quantum information processing. Here we report a different formulation of the master equation, describing dynamics beyond the linear response regime, where the drive induces additional damping in the system. We show that the equilibrium fluctuations of the thermal bath, in the form of Gaussian white noise processes, impart a finite memory to the state functions in our iterative expansion of the dynamical equation. This memory renders the nonlinear response terms time-nonlocal, in a suitably coarse-grained time-scale. In the context of an ensemble of spin qubits, we derive a modified form of Bloch equations having the leading order non-linear response terms and verify their existence experimentally. Since fluctuations are ineradicable in physical systems, our results indicate that manipulation of a qubit ensemble with external drives introduces unwanted damping, resulting in further loss of information.

PACS numbers: 05.30.d, 05.70.Ln, 05.40.-a, 76.60.-k, 03.67.a

arXiv:1703.01954v1 [quant-ph] 6 Mar 2017

I. INTRODUCTION

The use of quantum master equations (ME) for weakly coupled systems is well-spread, notably in various resonance spectroscopies and in experimental realization of ensemble quantum computing [1–4]. The traditional system plus bath models seek to derive an ME to describe the non-unitary behavior of the system by tracing out the bath degrees of freedom [1, 5–7]. Though the MEs typically involve a second-order perturbative expansion of the system-bath coupling, the application of any external drive on the system is usually treated in the linear response regime [1, 8–10]. A parallel approach assumes that the coupling and the drive induce independent rates of variation in the system resulting in a unitary evolution due to the drive [5, 7]. Therefore the system-bath coupling remains the only source of damping and hence non-unitary behavior in such systems. On the contrary, the semi-classical theory of Bloembergen, Purcell and Pound hints at the existence of nonlinear response terms in the MEs which lead to additional damping of the population differences [11]. Other semi-classical models used to explain the phenomenon of saturation also indicate the presence of higher order terms of the drive [12–15]. But the existing prescriptions to derive MEs are not well-suited to obtain time-nonlocal higher-order contributions of the drive.

Here we attempt to resolve this conflict by considering the finite memory effects of the bath originating from the equilibrium fluctuations of its energy levels. The bath-memory renders the higher order perturbations of the drive to be time-nonlocal and therefore opens up the possibility of a perturbative expansion up to any desired order. Restricting ourselves upto second-order, we subsequently derive a modified form of the Bloch equations having drive-induced damping terms and also provide a direct experimental verification of its validity.

II. THEORETICAL

To begin with, we consider an ensemble, each member of which is described by the following Hamiltonian in the angular frequency unit

$$\mathcal{H}(t) = \mathcal{H}_\circ^S + \mathcal{H}_\circ^L + \mathcal{H}^{SL} + \mathcal{H}^S(t) + \mathcal{H}^L(t), \qquad (1)$$

where, $\mathcal{H}_\circ^S$ and $\mathcal{H}_\circ^L$ represent the static Hamiltonians of the relevant and the non-relevant degrees of freedom respectively, which are weakly coupled by the term $\mathcal{H}^{SL}$. The collection of the relevant degrees of freedom constitute our system of interest whereas the non-relevant degrees of freedom together form a heat bath. $\mathcal{H}^S(t)$ denotes the external drive to the system. It is assumed that the bath is in thermal equilibrium at an inverse temperature β and experiences equilibrium fluctuations $\mathcal{H}^L(t)$, which solely act on the bath. $\mathcal{H}^L(t)$ may assume different values for different ensemble members while respecting the constraints imposed by the requirement of sustained thermal equilibrium. Apart from $\mathcal{H}^L(t)$, the other terms in the Hamiltonian are identical for all ensemble members and as such $\mathcal{H}_\circ^L$ determines the equilibrium density matrix of the bath. Since the fluctuations do not drive the bath away from equilibrium, we choose $\mathcal{H}^L(t)$ to be diagonal in the eigen-basis $\{|\phi_j\rangle\}$ of $\mathcal{H}_\circ^L$, represented by $H^L(t) = \sum_j f_j(t)|\phi_j\rangle\langle\phi_j|$. $f_j(t)$-s are assumed to be independent, Gaussian, δ-correlated stochastic variables with zero mean and standard deviation κ_j. We further assume that the fluctuation $\mathcal{H}^L(t)$

* arnab1106@iiserkol.ac.in
† rangeet@iiserkol.ac.in

and the state experiencing it at the time instant t are statistically independent so as to preserve causality.

Starting with this description, we perform all subsequent calculations in the interaction representation of $\mathcal{H}_\circ^S + \mathcal{H}_\circ^L$ and all Hamiltonians in this representation are denoted by H with relevant superscripts. Dynamics of a chosen member of the ensemble, denoted by $|\psi(t)\rangle$ in this representation, is described by the Liouville-von Neumann equation:

$$\partial_t\big(|\psi(t)\rangle\langle\psi(t)|\big) = -\mathrm{i}\Big[H^{\rm all}(t), |\psi(t)\rangle\langle\psi(t)|\Big], \quad (2)$$

where $H^{\rm all}(t) = H^{SL}(t) + H^S(t) + H^L(t)$. To derive an ME for the system we first take trace over the irrelevant degrees of freedom from both sides of the above equation and then perform a desired number of iterative substitutions using the integral form of the Schrödinger equation, $|\psi(t_1)\rangle = |\psi(t)\rangle - \mathrm{i}\int_t^{t_1} dt' H^{\rm all}(t')|\psi(t')\rangle$, $t_1 \geq t$. (Appendix: A). The main motivation behind adopting this iterative procedure is to capture the effect of a finite memory in the irrelevant part of the state function due to the fluctuations. We thus have

$$\begin{aligned}
\partial_{t_1}\Big(\mathrm{Tr_L}\Big\{|\psi(\mathrm{t_1})\rangle\langle\psi(\mathrm{t_1})|\Big\}\Big) = &-\mathrm{i}\,\mathrm{Tr_L}\Big[H^{\rm eff}(t_1), |\psi(t)\rangle\langle\psi(t)|\Big] - \int_t^{t_1} dt'\,\mathrm{Tr_L}\Big\{H^{\rm eff}(t_1)H^{\rm eff}(t')|\psi(t')\rangle\langle\psi(t)|\\
&- H^{\rm eff}(t')|\psi(t')\rangle\langle\psi(t_1)|H^{\rm eff}(t_1) - H^{\rm eff}(t_1)|\psi(t_1)\rangle\langle\psi(t')|H^{\rm eff}(t')\\
&+ |\psi(t_1)\rangle\langle\psi(t')|H^{\rm eff}(t')H^{\rm eff}(t_1)\Big\} - \int_t^{t_1} dt'\,\mathrm{Tr_L}\Big[H^{\rm eff}(t), \Big[H^L(t'), |\psi(t')\rangle\langle\psi(t')|\Big]\Big]\\
&+ \mathrm{i}\int_t^{t_1} dt' \int_t^{t_1} dt'' \mathrm{Tr_L}\Big[H^{\rm eff}(t), H^{\rm eff}(t_2)|\psi(t_2)\rangle\langle\psi(t_1)H^L(t_1)\Big]\\
&+ \mathrm{i}\int_t^{t_1} dt' \int_t^{t_1} dt'' \mathrm{Tr_L}\Big[H^{\rm eff}(t), H^L(t_1)|\psi(t_1)\rangle\langle\psi(t_2)H^{\rm eff}(t_2)\Big] + \mathcal{O}[(H^{\rm eff})^3(t)], \qquad (3)
\end{aligned}$$

where $H^{\rm eff}(t) = H^{SL}(t) + H^S(t)$.

Averaging over the ensemble while using the statistical properties of $H^L(t)$, then results in a dynamical equation for the system, involving the effective Hamiltonian $H^{\rm eff}(t)$ and terms of the form $\big\langle|\psi(t_1)\rangle\langle\psi(t_2)|\big\rangle$ in second and higher orders of $H^{\rm eff}(t)$, where, the angular brackets denote ensemble average (Appendix: B). Usually the largest time-scales associated with the correlation of the bath variables (τ_c) is much smaller than that of the system τ_s which is determined by $H^{\rm eff}(t)$. As such, there exists two widely different time-scales in this problem which allows a coarse-graining over the time interval $[t, t+\Delta t]$, such that $\tau_c \ll \Delta t \ll \tau_s$. The second order terms in $H^S(t)$ as well as $H^{SL}(t)$ are smaller than the first order terms as long as such a time-scale separation exists in the problem. Third and higher order terms are successively smaller by factors of $|H^{\rm eff}(t)|\tau_c \ll 1$ or $|H^{\rm eff}(t)|\Delta t \ll 1$. Hence we neglect terms $\mathcal{O}[(H^{\rm eff})^{3+}(t)]$ for a sufficiently weak drive and coupling [7].

In order to evaluate $\big\langle|\psi(t_1)\rangle\langle\psi(t_2)|\big\rangle$ $\forall t \leq t_1, t_2 \leq t+\Delta t$, we use the time-ordered propagator generated only by $H^L(t)$, since in the time-scale of the course-grain interval, only the bath fluctuations are significant. This, in essence is similar to the Markov approximation, whereby one neglects the time evolution of the system in the second-order term of the ME, within the short duration Δt [5, 7]. Any back-action of the system dynamics to the bath via the coupling is avoided by this protocol.

To obtain expressions in a familiar closed form we ascribe an identical standard deviation κ to all $f_j(t)$-s. Assuming that at the beginning of the coarse-grain interval, the density matrix for the whole ensemble can be factorized into that of the system and the bath with the latter at thermal equilibrium, we obtain

$$\Big\langle|\psi(t_1)\rangle\langle\psi(t_2)|\Big\rangle = \rho_S(t)\otimes\rho_L^{\rm eq}\exp\big(-\kappa^2|t_1-t_2|\big), \quad (4)$$

where $\rho_S(t)$ denotes the density matrix of the system whereas $\rho_L^{\rm eq}$ denotes the equilibrium density matrix of the heat bath (Appendix: C). Using the above result we find that the integrand in the second order term of the coarse-grained equation takes the form of a double commutator decaying within the time-scale of $1/\kappa^2$. Thus $1/\kappa^2$ forms the upper bound of the time-scales during which the bath correlations are significant and as such we replace it by τ_c. Following the prescription of Cohen-Tannoudji *et.al.*, we then arrive at the following ME:

$$\partial_t \rho_S(t) = -\mathrm{i}\,\mathrm{Tr_L}\Big[H^{\mathrm{eff}}(t), \rho_S(t)\otimes\rho_L^{eq}\Big]^{\mathrm{sec}} - \int_0^\infty d\tau\ \mathrm{Tr_L}\Big[H^{\mathrm{eff}}(t), \Big[H^{\mathrm{eff}}(t-\tau), \rho_S(t)\otimes\rho_L^{eq}\Big]\Big]^{\mathrm{sec}} e^{-|\tau|\tau_c}, \tag{5}$$

where, the superscript 'sec' denotes that only the secular contributions are retained (ensured by the coarse graining) and $\mathrm{Tr_L}$ denotes the partial trace. Unlike the usual forms of ME found in literature, equation (5) has a finite, time-nonlocal, second-order contribution of the external drive to the system [5, 7–10, 13]. The derived ME (5) yields Lorenztian spectral density functions due to the presence of the exponential decay term. While the equation ensures that the system approaches equilibrium, the specific form of the equilibrium distribution is determined by the resonance condition (Appendix: D).

As a practical example, we now consider our system to be the spin degrees of freedom of an ensemble of isolated spin 1/2 nuclei (qubits) embedded in solute molecules of a dilute liquid solution placed in a static external magnetic field, the direction of which is chosen to define our $\hat{z}$ axis. The spatial degrees of freedom relevant in this problem constitute an isotropic thermal bath at an inverse temperature β. The system is also subjected to a weak, near-resonant magnetic field (the drive) of strength ω_1 along $\hat{x}$, oscillating with a frequency ω. In a typical NMR measurement, heterodyne detection is performed followed by low-pass filtering, which is equivalent to measurements made in a co-rotating frame of frequency ω [16]. Hence we suitably define the macroscopic magnetization components $M_\alpha(t)$ $\alpha \in \{x, y, z\}$. Using the ME (5) along with the assumption of isotropicity *i.e.* $\mathrm{Tr_L}[H^{SL}(t), \rho_S(t)\otimes\rho_L^{eq}] = 0$, we arrive at a modified form of the Bloch equations for $M_\alpha(t)$:

$$\begin{aligned}
\dot{M}_z &= \omega_1 M_y - \frac{1}{T_1}(M_z - M_\circ) - \frac{\omega_1^2\tau_c}{1+\Delta\omega^2\tau_c^2}M_z,\\
\dot{M}_x &= \Delta\omega M_y - \frac{1}{T_2}M_x,\\
\dot{M}_y &= -\Delta\omega M_x - \omega_1 M_z - \frac{1}{T_2}M_y - \frac{\omega_1^2\tau_c}{1+\Delta\omega^2\tau_c^2}M_y
\end{aligned} \tag{6}$$

where, $\Delta\omega = \omega - \omega_\circ$ is the offset from the resonance frequency $\omega_\circ$, T_1, T_2 are the longitudinal and transverse relaxation times respectively and $M_\circ$ is the equilibrium magnetization [1, 5, 7]. In deriving the above equations we have neglected the counter-rotating components of the driving field and also all Lamb shift terms [5, 7, 16] (Appendix: E). The additional terms in the equations (6) proportional to $\omega_1^2\tau_c$ lead to a faster approach to saturation in conformity with [11, 15]. If $\omega_1^2\tau_c \ll 1/T_1, 1/T_2$, *i.e.* at high motional-narrowing limit, these extra terms become negligible and thereby we recover the original Bloch equations.

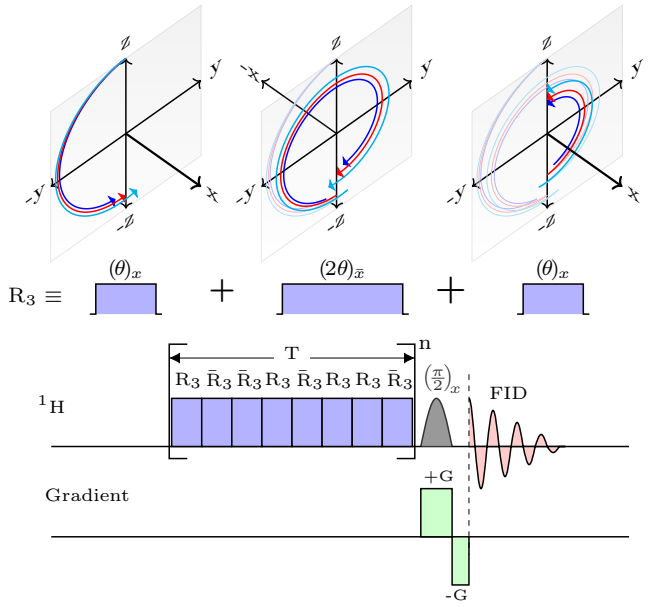

FIG. 1. Schematic representation of the refocusing scheme and the pulse sequence used in the experiment. R_3 is equivalent to an on-resonance 3-pulse block composed of $\theta, 2\theta, \theta$ pulses along $\hat{x}, -\hat{x}, \hat{x}$ respectively with $\theta \sim \pi$. $\bar{x}$ in the figure denotes the drive applied along $-\hat{x}$. The 3D diagrams atop the pulses show how the refocusing happens irrespective of the actual value of the flip angle θ and hence ω_1. The pulse sequence below shows the operations performed on the proton (^{1}H) and the gradient channels respectively. After a recycle delay of $10\,\mathrm{s}(> 6T_1)$, we employ a super-cycle of R_3 inspired by WALTZ-8 as the drive sequence [17]. $\bar{\mathrm{R}}_3$ indicates all pulses in R_3 are applied along inverted axis. $[\,]^n$ implies that the sequence within the brackets is repeated n times consecutively and T denotes the length of a super-cycle. For detection, we have applied a Gaussian selective pulse of flip angle $\sim \pi/2$ in the presence of the applied gradient +G to facilitate slice selection using spatial encoding. Immediately after the slice selection, an opposite compensatory gradient −G is used to minimize phase distortion during slice-selection [18]. The Free Induction Decay (FID) has been recorded in the absence of any gradient. Magnetization, M_z is measured from the FID as a function of n. From the M_z versus nT data we measure R_z using least-square curve fit.

III. EXPERIMENTAL

The resonance condition $\Delta\omega = 0$ decouples the dynamics of M_x from that of M_y and M_z. When $\omega_1 > 1/T_1, 1/T_2$, we get a damped nutation in the yz-plane, starting from $\hat{z}$. The nutation frequency is $\sqrt{\omega_1^2 + \frac{1}{4}(1/T_2 - 1/T_1)^2} \simeq \omega_1$ and the damping rate is

$(T_1+T_2)/2T_1T_2+\omega_1^2\tau_c$. Since τ_c is of the order of 'ps' in liquids and typically $\omega_1 \sim$kHz, the term $\omega_1^2\tau_c$ is usually small in comparison to $(T_1+T_2)/2T_1T_2$ [23–25]. Thus in order to observe its effect, we drive the system for long enough times (of the order of 100 ms).

The drive strength, ω_1 is not entirely homogeneous throughout the sample volume in practical cases. This leads to an additional decay of the measured signal due to the fanning out of the magnetization components in the yz-plane. Usually the measured decay of nutation is dominated by this first-order dephasing, due to the presence of drive-inhomogeneity in the sample, which obscures the ω_1^2 dependence of the damping rate. To avoid this we adopt a refocusing scheme so that $\omega_1 t = 0$ at every instant of measurement t. Under these assumptions we have a solution of the form $M_z(t) = a + b\exp[-R_z t]$ and $M_y(t) = 0$, where $R_z = (T_1+T_2)/2T_1T_2 + \omega_1^2\tau_c$, a and b are functions of M_o, T_1, T_2, ω_1 and τ_c. So we measure the decay rates, R_z at various drive strengths, ω_1 to establish the quadratic dependence of the former on the latter.

An efficient refocusing process should aim to make $M_y(t)$ as small as possible at each measuring instant t. The simplest possible method to accomplish this involves the application of a continuous train of pulses with flip-angles θ and $-\theta$ (i.e. $\omega_1 t = \theta, -\theta$) alternately with measurements made after even number of pulses. Nutation by an angle $-\theta$ is achieved by applying the drive along $-\hat{x}$. Since after an even number of pulses in the sequence, the net phase of the nutating magnetization components become zero, the resulting dynamics remains immune to the drive inhomogeneity-induced dephasing. We choose $\theta \sim \pi$ for our experiments to minimize precession about $\hat{z}$ (if any, due to incorrect shim profile) which takes the magnetization out of the yz-plane (during the finite rise and fall times of the pulses). The 3-pulse block, $\mathrm{R}_3 = \{\pi, -2\pi, \pi\}$ is more efficient than the simple $\mathrm{R}_2 = \{\pi, -\pi\}$ block in minimizing the y-leakage, $M_y(t)$. This can be verified by calculating the ratio of the leakage magnetizations, $M_y^{\mathrm{R}_3}(t)/M_y^{2\mathrm{R}_2}(t)$ obtained by running the two sequences for the same duration, $t = 4\pi/\omega_1$ (i.e. R_2 is run twice consecutively while R_3 is run only once). This ratio turns out to be $-\tanh[\pi\{1/T_1 + 1/T_2 + 2\omega_1^2\tau_c\}/2\omega_1]$. Now, $\omega_1 > 1/T_1, 1/T_2$ and $\omega_1^2\tau_c \ll (T_1+T_2)/2T_1T_2$ as mentioned before and since for small θ, $\tanh[\theta] \sim \theta$, the ratio $M_y^{\mathrm{R}_3}(t)/M_y^{2\mathrm{R}_2}(t)$ is negligible. Inspired by the WALTZ-8 decoupling scheme, we find, through simulations with $\tau_c \sim 10^{-12}$s, that the super-cycle $\mathrm{S} = \mathrm{R}_3\bar{\mathrm{R}}_3\bar{\mathrm{R}}_3\mathrm{R}_3\ \bar{\mathrm{R}}_3\mathrm{R}_3\mathrm{R}_3\bar{\mathrm{R}}_3$, (where $\bar{\mathrm{R}}_3 = \{-\pi, 2\pi, -\pi\}$) is more effective than the simple 3-pulse block R_3 in minimizing $M_y(t)$ and thus we use it as our driving protocol [17]. In order to further eliminate the effect of drive-inhomogeneity, we select a thin slice ($\sim$ 1 mm) near the middle of the sample (effective height $\sim$ 25 mm), for detection, by using a selective Gaussian $\pi/2$ pulse along $\hat{x}$ in presence of an applied z-gradient of about $0.05\mathrm{Tm}^{-1}$ [18, 19]. The duration of the positive gradient is 2 ms whereas that of the compensatory gradient is 1.1 ms. The experimental protocol is illustrated in FIG. 1.

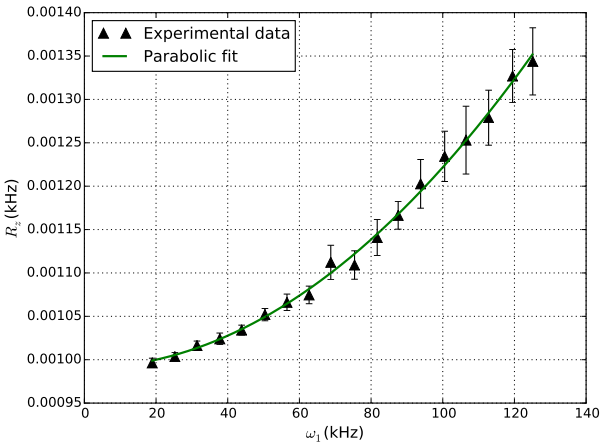

FIG. 2. Plot of the decay rate R_z versus the drive strength ω_1. The upright triangles denote the experimentally determined values of R_z with the vertical bars denoting the errors in the determination of R_z at 95% level of confidence. The solid line (color online) shows the parabolic fit of the experimental data.

To experimentally verify the equations (6), we choose the singlet imine protons in a dilute (mM) solution of N-(4′-methoxybenzylidene)-4-n-butylaniline in DMSO-D_6 placed in a static magnetic field along $\hat{z}$, as our target spin system. The application of an on-resonance ($\Delta\omega \to 0$) drive along $\hat{x}$, results in a damped nutation in the yz-plane (if $\omega_1 > 1/T_1, 1/T_2$), starting from $\hat{z}$, with a damping rate: $R_z = (T_1+T_2)/2T_1T_2 + \omega_1^2\tau_c$.

IV. RESULTS AN DISCUSSION

We have performed all experiments on a Bruker Avance III 11.78 T NMR spectrometer at 294 K. The drive strength $\omega_1/2\pi$ has been varied from 3 kHz to 20 kHz, in steps of 1 kHz. For each drive strength, we have determined the decay rate of nutation, R_z as a function of nutation period. A plot of R_z as a function of ω_1 is shown in Fig. 2.

The chemical shift of the chosen imine protons is $\sim$ 8.4ppm w.r.t. TMS [26]. The choice of the molecule is motivated by its relatively slow isotropic rotation in solution phase due to its long structure. The T_1 and T_2 relaxation times for our system, measured using standard techniques, are 1.34s and 0.81s respectively [20–22]. For each value of $\nu_1 = \omega_1/2\pi$, we drive the system n times, where n ranges from 1 to 121 in steps of 5, so that the maximum drive-time does not exceed 500ms. Thus for $\nu_1 = 3$kHz the maximum value of n is 91. For all other values of ν_1 we use the full range of n. This ensures that imperfections due to finite rise and fall times of the pulses

have nearly identical effects for each ν_1. While 20kHz is approximately close to the maximum power limit of the spectrometer, we do not go below the 3kHz limit simply because the drive time exceeds 500ms for a significantly small value of n compared to 121 thereby leading to distortions. We calculate M_z after each experimental run from the FID using Plancherel's Theorem [27]. Taking the natural logarithm of the time-series of M_z and fitting the result with a straight line we obtain R_z for a particular value of ω_1.

We note that our experimental protocol is sensitive to shim conditions and the accurate calibration of the drive power. In all the experiments we calibrate our pulses using the fact that a 1.3db pulse produces a nutation frequency of 14.25kHz. The success of the refocusing scheme also relies on minimal translational diffusion during R_3 which we presume to be the case since the duration of R_3 is of the order of tens of μs. The maximum drive strength used in our experiments is $\nu_1 = 20$kHz (close to the maximum permissible power) whereas the proton Larmor frequency of the spectrometer is of about 500MHz. Thus the second order approximation in our ME is valid for all practical considerations.

The R_z versus ω_1 data is fit with a parabola of the form $y = a_1 + b_1 x^2$ as shown in FIG. 2. From the fit we obtain the value of τ_c to be 2.31×10^{-11} s. The value of a_1 is found to be 0.99 Hz which is same as the value of $(T_1 + T_2)/2T_1T_2$ within experimental error, the latter being estimated using standard measurement techniques [20–22]. For the R_z versus ω_1^2 behavior, we find fair agreement between the theoretical prediction and the experimental observation. Hence we infer that our experimental results confirm the validity of the dynamical equations (6) obtained from our ME (5).

V. CONCLUSION

Our results reveal that the finite memory of the bath plays a central role in giving rise to an additional damping of Rabi oscillations in the form of a time-nonlocal nonlinear response of the system to the drive. Application of our formalism to magnetic resonance results in a modified form of Bloch equations having drive-induced damping terms. Since τ_c is a measure of the bath correlation times, such effects may become significant for systems coupled to thermal baths with large τ_c; the magnetic resonance of solid samples is a case in point. For liquids, such nonlinear effects are small and is usually obscured by the drive inhomogeneity. However a refocusing scheme which prevents the dephasing due to such inhomogeneities during nutation, helps confirm the existence of the nonlinear terms. At extreme motional-narrowing limit ($\tau_c \to 0$), the equations (6) predict an expected unitary nutation of the system due to the drive.

Our choice of δ-correlated fluctuations lead to an exponential memory function; although other noise models may also serve the purpose. Also, our assumption of identical standard deviations κ_j of the bath energy levels is not rigorous but it may be reasonable for the levels which are effectively coupled to the system. Since $\Delta\omega\tau_c \ll 1$, this damping becomes small for smaller τ_c and hence it is envisaged that a bath with stronger fluctuations (towards the extreme motional narrowing limit) would make the system more immune to drive-induced damping. Damping of this kind may pose a serious hindrance in the realization of long-time quantum information processing protocols in the context of ensemble computing.

Appendix A: Iterative expansion

Dynamics of a chosen member of the ensemble, denoted by $|\psi(t)\rangle$ in the interaction representation is described by the Liouville-von Neumann equation:

$$\partial_t\big(|\psi(t)\rangle\langle\psi(t)|\big) = -\mathrm{i}\Big[H^{\mathrm{all}}(t), |\psi(t)\rangle\langle\psi(t)|\Big], \qquad \text{(A1)}$$

where $H^{\mathrm{all}}(t) = H^{SL}(t) + H^S(t) + H^L(t)$. To describe the system dynamics, we take a partial trace over the irrelevant degrees of freedom on both sides of equation (A1). Since $H^L(t)$ is an operator on the irrelevant subspace, the partial trace removes its commutator in the r.h.s. of the equation (2) which then becomes $-\mathrm{i}\,\mathrm{Tr_L}\Big[H^{\mathrm{eff}}(t), |\psi(t)\rangle\langle\psi(t)|\Big]$, where $H^{\mathrm{eff}}(t) = H^{SL}(t) + H^S(t)$. $\mathrm{Tr_L}$ denotes the partial trace. Using the fact that $|\psi(t_1)\rangle = |\psi(t)\rangle - \mathrm{i}\int_t^{t_1} dt'\, H^{\mathrm{all}}(t')|\psi(t')\rangle$ for $t_1 \geq t$ we obtain

$$\begin{aligned}\partial_{t_1}\Big(\mathrm{Tr_L}\Big\{|\psi(t_1)\rangle\langle\psi(t_1)|\Big\}\Big) = -\mathrm{i}\,\mathrm{Tr_L}\Big[&H^{\mathrm{eff}}(t_1)|\psi(t_1)\rangle\langle\psi(t)| - |\psi(t_1)\rangle\langle\psi(t)|H^{\mathrm{eff}}(t_1) \\ &+\mathrm{i}\int_t^{t_1} dt' H^{\mathrm{eff}}(t_1)|\psi(t_1)\rangle\langle\psi(t')|H^{\mathrm{all}}(t') \\ &-\mathrm{i}\int_t^{t_1} dt'|\psi(t_1)\rangle\langle\psi(t')|H^{\mathrm{all}}(t')H^{\mathrm{eff}}(t_1)\Big]. \qquad \text{(A2)}\end{aligned}$$

Further expansion of the first-order terms in equation (A2) leads to the exact expression

$$\begin{aligned}\partial_{t_1}\Big(\mathrm{Tr_L}\Big\{|\psi(t_1)\rangle\langle\psi(t_1)|\Big\}\Big) &= -\mathrm{i}\,\mathrm{Tr_L}\Big[H^{\mathrm{eff}}(t_1),|\psi(t)\rangle\langle\psi(t)|\Big]\\ &-\int_t^{t_1} dt'\,\mathrm{Tr_L}\Big\{H^{\mathrm{eff}}(t_1)H^{\mathrm{all}}(t')|\psi(t')\rangle\langle\psi(t)| - H^{\mathrm{all}}(t')|\psi(t')\rangle\langle\psi(t)|H^{\mathrm{eff}}(t_1)\\ &- H^{\mathrm{eff}}(t_1)|\psi(t_1)\rangle\langle\psi(t')|H^{\mathrm{all}}(t') + |\psi(t_1)\rangle\langle\psi(t')|H^{\mathrm{all}}(t')H^{\mathrm{eff}}(t_1)\Big\}. \end{aligned} \tag{A3}$$

Substituting $\langle\psi(t)|$ in the integrand of equation (A3) by $\langle\psi(t_1)|$, using the integral form of the Schrödinger equation results in

$$\begin{aligned}\partial_{t_1}\Big(\mathrm{Tr_L}\Big\{|\psi(t_1)\rangle\langle\psi(t_1)|\Big\}\Big) &= -\mathrm{i}\,\mathrm{Tr_L}\Big[H^{\mathrm{eff}}(t_1),|\psi(t)\rangle\langle\psi(t)|\Big] - \int_t^{t_1} dt'\,\mathrm{Tr_L}\Big\{H^{\mathrm{eff}}(t_1)H^{\mathrm{eff}}(t')|\psi(t')\rangle\langle\psi(t_1)|\\ &- H^{\mathrm{eff}}(t')|\psi(t')\rangle\langle\psi(t_1)|H^{\mathrm{eff}}(t_1) - H^{\mathrm{eff}}(t_1)|\psi(t_1)\rangle\langle\psi(t')|H^{\mathrm{eff}}(t')\\ &+ |\psi(t_1)\rangle\langle\psi(t')|H^{\mathrm{eff}}(t')H^{\mathrm{eff}}(t_1)\Big\} - \int_t^{t_1} dt'\,\mathrm{Tr_L}\Big\{H^{\mathrm{eff}}(t_1)H^{L}(t')|\psi(t')\rangle\langle\psi(t_1)|\\ &- H^{L}(t')|\psi(t')\rangle\langle\psi(t_1)|H^{\mathrm{eff}}(t_1) - H^{\mathrm{eff}}(t_1)|\psi(t_1)\rangle\langle\psi(t')|H^{L}(t')\\ &+ |\psi(t_1)\rangle\langle\psi(t')|H^{L}(t')H^{\mathrm{eff}}(t_1)\Big\}\\ &+\mathrm{i}\int_t^{t_1} dt'\int_t^{t_1} dt''\mathrm{Tr_L}\Big\{H^{\mathrm{eff}}(t_1)H^{\mathrm{all}}(t')|\psi(t')\rangle\langle\psi(t'')|H^{\mathrm{all}}(t'')\Big\}\\ &-\mathrm{i}\int_t^{t_1} dt'\int_t^{t_1} dt''\mathrm{Tr_L}\Big\{H^{\mathrm{all}}(t')|\psi(t')\rangle\langle\psi(t'')|H^{\mathrm{all}}(t'')H^{\mathrm{eff}}(t_1)\Big\} \end{aligned} \tag{A4}$$

We note that the above equation is a finite-order expansion unlike the traditional Dyson series which extends to infinite orders. The third order terms in $H^{\mathrm{eff}}(t)$ are denoted by $\mathcal{O}[(H^{\mathrm{eff}})^3(t)]$. After some algebraic rearrangements we have from equation (A4),

$$\partial_{t_1}\Big(\mathrm{Tr_L}\Big\{|\psi(t_1)\rangle\langle\psi(t_1)|\Big\}\Big) = -\mathrm{i}\,\mathrm{Tr_L}\Big[H^{\mathrm{eff}}(t_1), |\psi(t)\rangle\langle\psi(t)|\Big] - \int_t^{t_1} dt'\,\mathrm{Tr_L}\Big\{H^{\mathrm{eff}}(t_1)H^{\mathrm{eff}}(t')|\psi(t')\rangle\langle\psi(t_1)|$$
$$-H^{\mathrm{eff}}(t')|\psi(t')\rangle\langle\psi(t_1)|H^{\mathrm{eff}}(t_1) - H^{\mathrm{eff}}(t_1)|\psi(t_1)\rangle\langle\psi(t')|H^{\mathrm{eff}}(t')$$
$$+|\psi(t_1)\rangle\langle\psi(t')|H^{\mathrm{eff}}(t')H^{\mathrm{eff}}(t_1)\Big\} - \int_t^{t_1} dt'\,\mathrm{Tr_L}\Big[H^{\mathrm{eff}}(t), \Big[H^L(t'), |\psi(t')\rangle\langle\psi(t')|\Big]\Big]$$
$$+\mathrm{i}\int_t^{t_1} dt' \int_t^{t_1} dt''\mathrm{Tr_L}\Big[H^{\mathrm{eff}}(t), H^{\mathrm{eff}}(t_2)|\psi(t_2)\rangle\langle\psi(t_1)H^L(t_1)\Big]$$
$$+\mathrm{i}\int_t^{t_1} dt' \int_t^{t_1} dt''\mathrm{Tr_L}\Big[H^{\mathrm{eff}}(t), H^L(t_1)|\psi(t_1)\rangle\langle\psi(t_2)H^{\mathrm{eff}}(t_2)\Big] + \mathcal{O}[(H^{\mathrm{eff}})^3(t)]. \tag{A5}$$

Appendix B: Ensemble average and the causality requirements

Averaging both sides of equation (A5) over the whole ensemble while using the assumptions that $H^L(t')$ is statistically independent of $|\psi(t')\rangle$, $|\psi(t)\rangle$ $\forall t \leq t'$ and $\langle H^L(t')\rangle = 0$ we obtain

$$\partial_{t_1}\rho_S(t_1) = -\mathrm{i}\,\mathrm{Tr_L}\Big[H^{\mathrm{eff}}(t_1), \rho(t)\Big] - \int_t^{t_1} dt'\,\mathrm{Tr_L}\Big\{H^{\mathrm{eff}}(t_1)H^{\mathrm{eff}}(t')\Big\langle|\psi(t')\rangle\langle\psi(t_1)|\Big\rangle$$
$$-H^{\mathrm{eff}}(t')\Big\langle|\psi(t')\rangle\langle\psi(t_1)|\Big\rangle H^{\mathrm{eff}}(t_1) - H^{\mathrm{eff}}(t_1)\Big\langle|\psi(t_1)\rangle\langle\psi(t')|\Big\rangle H^{\mathrm{eff}}(t')$$
$$+\Big\langle|\psi(t_1)\rangle\langle\psi(t')|\Big\rangle H^{\mathrm{eff}}(t')H^{\mathrm{eff}}(t_1)\Big\} + \mathcal{O}[(H^{\mathrm{eff}})^3(t)], \tag{B1}$$

where $\rho_S(t_1) = \mathrm{Tr_L}[\rho(t_1)] = \mathrm{Tr_L}[\langle|\psi(t_1)\rangle\langle\psi(t_1)|\rangle]$ and ρ_S and ρ denote the density matrices of the system alone and that of the combined system and bath respectively.

Appendix C: Emergence of the memory of the bath from the fluctuations

Following Cohen-Tannoudji *et.al.* we define a coarse-grained version of equation (B1) for the time-span $[t, t+\Delta t]$, such that $\tau_c \ll \Delta t \ll \tau_s$, by approximating the instantaneous rate $\partial_t\rho_S(t)$ by the coarse-grained rate $\partial_t^{\mathrm{CG}}\rho_S(t) = \big[\rho_S(t+\Delta t) - \rho_S(t)\big]/\Delta t$. Integrating (B1) w.r.t. t_1 between the limits $[t, t+\Delta t]$ and dividing both sides by Δt, while replacing the dummy-variable t' with t_2, we obtain the coarse-grained master equation [7].

$$\partial_t^{\mathrm{CG}}\rho_S(t_1) = \frac{1}{\Delta t}\Big\{\rho_S(t+\Delta t) - \rho_S(t)\Big\}$$
$$= -\mathrm{i}\frac{1}{\Delta t}\int_t^{t+\Delta t} dt_1\mathrm{Tr_L}\Big[H^{\mathrm{eff}}(t_1), \rho(t)\Big] - \frac{1}{\Delta t}\int_t^{t+\Delta t} dt_1 \int_t^{t_1} dt_2\,\mathrm{Tr_L}\Big\{H^{\mathrm{eff}}(t_1)H^{\mathrm{eff}}(t_2)\Big\langle|\psi(t_2)\rangle\langle\psi(t_1)|\Big\rangle$$
$$-H^{\mathrm{eff}}(t_2)\Big\langle|\psi(t_2)\rangle\langle\psi(t_1)|\Big\rangle H^{\mathrm{eff}}(t_1) - H^{\mathrm{eff}}(t_1)\Big\langle|\psi(t_1)\rangle\langle\psi(t_2)|\Big\rangle H^{\mathrm{eff}}(t_2)$$
$$+\Big\langle|\psi(t_1)\rangle\langle\psi(t_2)|\Big\rangle H^{\mathrm{eff}}(t_2)H^{\mathrm{eff}}(t_1)\Big\} + \mathcal{O}[(H^{\mathrm{eff}})^3(t)], \tag{C1}$$

Together with the weak-coupling assumption we also assume that the drive to the system, $H^S(t)$, is weak such that the terms of third and higher order in $H^{\rm eff}(t)$ become negligible if Δt is much shorter than the time scales associated with $H^{\rm eff}(t)$ (denoted by τ_s). Since $\Delta t \ll \tau_s$, we can neglect the time-evolution due to $H^{\rm eff}(t)$ between $|\psi(t)\rangle$ and $|\psi(t+\Delta t)\rangle$ in the second-order terms of the coarse-grained version equation (C1) and also the terms $\mathcal{O}[(H^{\rm eff})^3(t)]$.

Assuming that at the beginning of the coarse-graining interval the full density matrix has the factorised form $\rho(t) = \rho_S(t) \otimes \rho_L^{\rm eq}$, where $\rho_L^{eq} = \exp(-\beta \mathcal{H}_\circ^L)/\mathcal{Z}_L$ denotes the equilibrium density matrix of the bath, $\mathcal{Z}_L$ being the partition function, we use the usual time ordered propagator $U_L(t_1, t)$ due to $H^L(t)$ to obtain

$$\begin{aligned}\Big\langle |\psi(t_1)\rangle\langle\psi(t_2)| \Big\rangle &= \Big\langle U_L(t_1,t)|\psi(t)\rangle\langle\psi(t)|U_L^\dagger(t_2,t)\Big\rangle \\ &= \rho_S(t) \otimes \sum_j \frac{e^{-\beta\omega_j}}{\mathcal{Z}_L} |\phi_j\rangle\langle\phi_j| \Big\langle \exp\big\{ -\mathrm{i}\int_t^{t_1} dt'\, f_j(t') + \mathrm{i}\int_t^{t_2} dt''\, f_j(t'')\big\}\Big\rangle \\ &= \rho_S(t) \otimes \sum_j \frac{e^{-\beta\omega_j}}{\mathcal{Z}_L} |\phi_j\rangle\langle\phi_j| \exp\big(-\kappa_j^2 |t_1 - t_2|\big). \end{aligned} \tag{C2}$$

In the above expression ω_j denotes the eigen-value of $\mathcal{H}_\circ^L$ corresponding to $|\phi_j\rangle$ and we have made use of the fact that $H^L(t)$ and thus the propagators $U_L(t_1,t)$ are independent of the initial distribution of the bath states. To obtain expressions in a familiar closed form we assume that all $f_j(t)$-s have an identical variance, κ.

Thus we obtain

$$\Big\langle |\psi(t_1)\rangle\langle\psi(t_2)| \Big\rangle = \rho_S(t) \otimes \rho_L^{\rm eq} \exp\big(-\kappa^2 |t_1 - t_2|\big). \tag{C3}$$

Appendix D: Arriving at the Master Equation and the thermal equilibrium of the system

Substituting (C3) in the coarse-grained equation (C1), we observe that the second order term takes the form of a double-commutator decaying within the time-scale of $1/\kappa^2$. Thus $1/\kappa^2$ forms the upper bound of the time-scales during which the bath correlations are significant and as such we replace it by τ_c. Finally, following the prescription of Cohen-Tannoudji *et.al.* we remove the non-secular contributions by averaging over the coarse-grained time-span, Δt and approximate the coarse-grained derivative of $\rho_S(t)$ by its ordinary partial derivative to obtain the quantum master equation (ME):

$$\begin{aligned}\partial_t \rho_S(t) = &-\mathrm{i}\,\mathrm{Tr_L}\Big\{\Big[H^{\rm eff}(t), \rho_S(t)\otimes\rho_L^{eq}\Big]^{\rm sec}\Big\} \\ &- \int_0^\infty d\tau\, \mathrm{Tr_L}\Big\{\Big[H^{\rm eff}(t), \Big[H^{\rm eff}(t-\tau), \rho_S(t)\otimes\rho_L^{eq}\Big]\Big]^{\rm sec}\Big\} e^{-\frac{|\tau|}{\tau_c}}. \end{aligned} \tag{D1}$$

where, the superscript 'sec' denotes that only secular contributions are retained [7]. Here we have replaced Δt in the upper limit of the integral in equation (D1) with ∞, since the integrand decays within the short time span $\tau_c \ll \Delta t$, irrespective of the form of the perturbation, $H^{\rm eff}(t)$ [5, 7].

Approach to Thermal Equilibrium– To show that ME (D1) predicts approach to thermal equilibrium for the system density matrix, $\rho_S(t)$, in the absence of an external drive, $H^S(t)$, we follow the analysis of Cohen-Tannoudji *et.al.* with suitable modifications [7]. Defining the coupling Hamiltonian as $\mathcal{H}^{SL} = \mathcal{A} \otimes \mathcal{R}$, ($\mathcal{A}$ and $\mathcal{R}$ are Hermitian operators on the relevant and irrelevant subspaces respectively) we express the ME (D1) in the eigen-basis of $\mathcal{H}_\circ^S$ assuming the Bohr frequencies of the system to be non-degenerate [7]. The dissipator of the resulting equation involves bath spectral-densities of the

form (ignoring Lamb shifts [5])

$$J(\omega) = \frac{1}{2}\int\limits_{-\infty}^{\infty} d\tau\, e^{\mathrm{i}\omega\tau}\mathrm{Tr}_{\mathrm{L}}\Big[R(\tau)R(0)\rho_L^{eq}\Big]e^{-\frac{|\tau|}{\tau_c}}$$
$$= \frac{1}{2}\int\limits_{-\infty}^{\infty} d\tau \sum_j \frac{e^{-\beta\omega_j}}{\mathcal{Z}_L}\sum_k e^{\mathrm{i}(\omega+\omega_{jk})\tau}|\mathcal{R}_{jk}|^2 e^{-\frac{|\tau|}{\tau_c}} \tag{D2}$$

and

$$K(-\omega) = \frac{1}{2}\int\limits_{-\infty}^{\infty} d\tau\, e^{-\mathrm{i}\omega\tau}\mathrm{Tr}_{\mathrm{L}}\Big[R(\tau)R(0)\rho_L^{eq}\Big]e^{-\frac{|\tau|}{\tau_c}}, \tag{D3}$$

where $\omega_{jk} = \omega_j - \omega_k$, $\mathcal{R}_{jk} = \langle\phi_j|\mathcal{R}|\phi_k\rangle$, ω denotes the energy gap (in angular frequency units) between any two levels of the system (Bohr frequency) and $R(\tau)$ is the interaction representation of $\mathcal{R}$. Then it suffices to show that $K(-\omega) = \exp(-\beta\omega)J(\omega)$ [5]. To this end we have,

$$K(-\omega) = \frac{1}{2}\int\limits_{-\infty}^{\infty} d\tau \sum_j \frac{e^{-\beta\omega_j}}{\mathcal{Z}_L}\sum_k e^{\mathrm{i}(-\omega+\omega_{jk})\tau}|\mathcal{R}_{jk}|^2 e^{-\frac{|\tau|}{\tau_c}}$$
$$= \sum_{j,k} e^{-\beta\omega_{jk}}\frac{e^{-\beta\omega_k}}{\mathcal{Z}_L}|\mathcal{R}_{jk}|^2\frac{\tau_c}{1+(-\omega+\omega_{jk})^2\tau_c^2}. \tag{D4}$$

The Lorentzian form thus obtained in the above expression suggests that the maximum contribution to $K(-\omega)$ occurs when $\omega = \omega_{jk}$. For $1/\tau_c \ll \omega$ the width of the Lorentzian becomes very small and as such we can replace $e^{-\beta\omega_{jk}}$ in the above by $e^{-\beta\omega}$ and take it out of the summation. Following the usual method of analysis, we then obtain $K(-\omega) = e^{-\beta\omega}J(\omega)$ [7]. On the contrary when $1/\tau_c \gg \omega$, the Lorentzian has an appreciable contribution in the range $\omega - 1/\tau_c \le \omega_{jk} \le \omega + 1/\tau_c$. Even then the maximum contribution to the spectral densities occurs when $\omega_{jk} = \omega$. In any case, approach to an equilibrium distribution of the system is assured by the ME, although it may not always be possible to calculate a closed form expression of that distribution.

Appendix E: Derivation of the modified Bloch equations

To describe the dynamics of the spin $\frac{1}{2}$ system, we assume the Zeeman Hamiltonian, $H_\circ^S = \omega_\circ\mathcal{I}_z$ and the drive, $\mathcal{H}^S(t) = 2\omega_1\cos(\omega t)\mathcal{I}_x$, where $\omega_\circ$ is the resonance frequency of the spin-1/2 nuclei and $\mathcal{I}_\alpha$, $\alpha \in \{x, y, z\}$ denote the Cartesian components of the spin angular momentum operator. Since the drive is assumed to be near resonance, we have $\omega \sim \omega_\circ$. We do not ascribe any specific form to the coupling Hamiltonian, $\mathcal{H}^{SL}$ but following the usual practice, for an isotropic heat bath, we assume that $\mathrm{Tr}_{\mathrm{L}}[H^{SL}(t), \rho_S(t)\otimes\rho_L^{eq}] = 0$, which in turn ensures that the cross-terms between the drive and the coupling vanish identically in the second-order [1, 5, 7]. We consider the effects of the coupling only through relaxation terms proportional to $1/T_1$ and $1/T_2$ (T_1 and T_2 denote the longitudinal and transverse relaxation times respectively) [1]. A detailed derivation of the relaxation terms will be presented elsewhere. The perturbative regime, $\omega_1 \ll \omega_\circ \sim \omega$, allows us to neglect the rapidly fluctuating counter-rotating terms of the drive to get $H^S(t) = (\omega_1/2)[\mathcal{I}_+e^{-\mathrm{i}\Delta\omega t} + \mathcal{I}_-e^{\mathrm{i}\Delta\omega t}]$ in the interaction picture, where $\Delta\omega = \omega - \omega_\circ$ and $\mathcal{I}_\pm = \mathcal{I}_x \pm \mathrm{i}\mathcal{I}_y$ [16]. Since the heterodyne detection followed by low-pass filtering in a typical NMR measurement is equivalent to measurements made in a co-rotating frame of frequency ω, the macroscopic magnetization components are defined by

$$M_\alpha(t) = \mathrm{Tr}_{\mathrm{S}}[\rho_S(t)e^{-\mathrm{i}\Delta\omega t\mathcal{I}_z}\mathcal{I}_\alpha e^{\mathrm{i}\Delta\omega t\mathcal{I}_z}], \tag{E1}$$

where Tr_{S} denotes trace over the system degrees of freedom [16]. With these assumptions, the ME (D1) yields the following dynamical equations for the measured macroscopic magnetization components after ignoring any Lamb shift terms:

$$\dot{M}_z = \omega_1 M_y - \frac{1}{T_1}(M_z - M_\circ) - \frac{\omega_1^2\tau_c}{1+\Delta\omega^2\tau_c^2}M_z,$$
$$\dot{M}_x = \Delta\omega M_y - \frac{1}{T_2}M_x,$$
$$\dot{M}_y = -\Delta\omega M_x - \omega_1 M_z - \frac{1}{T_2}M_y - \frac{\omega_1^2\tau_c}{1+\Delta\omega^2\tau_c^2}M_y, \tag{E2}$$

where $M_\circ$ is the equilibrium value of the magnetization. The resonance offset, $\Delta\omega$ is very small in practical cases, so that $\Delta\omega\Delta t$ is not much greater than 1. Hence the secular approximation retains all the terms in the second-order of the drive. The dynamical equations (E2) clearly demonstrate that in the presence of a transverse drive, there exists additional terms quadratic in the drive strength, which in turn lead to faster journey to saturation [11, 15]. The equations (E2) become identical to the Bloch equations when $\omega_1^2\tau_c$ is negligible compared to $1/T_1, 1/T_2$, which is usually the case in most of the solution state NMR experiments.

[1] R. K. Wangsness and F. Bloch, Phys. Rev. **89**, 728, (1953).

[2] R. G. DeVoe and R. G. Brewer, Phys. Rev. Lett. **50**, 1269, (1983).

[3] Y. Zheng and F. L. H. Brown, Phys. Rev. Lett. **90**, 238305, (2003).

[4] N. A. Gershenfeld and I. L. Chuang, Science **275**, 350, (1997).

[5] H. -P. Breuer and F. Petruccione, *The Theory of Open Quantum Systems* (Oxford, New York, 2002), Chap. 3.

[6] U. Weiss, *Quantum Dissipative Systems* (World Scientific, Singapore, 2008), Chap. 3.

[7] C. Cohen-Tannoudji, J. Dupont-Roc and G. Gilbert, *Atom-Photon Interactions: Basic Processes and Applications* (WILEY-VCH, Germany, 2004), Chap. 4 and 5.

[8] F. Bloch, Phys. Rev. **102**, 104, (1955).

[9] F. Bloch, Phys. Rev. **105**, 1206, (1957).

[10] P. N. Argyres and P. L. Kelley, Phys. Rev. **134**, A98, (1963).

[11] N. Bloembergen, E. M. Purcell and R. V. Pound, Phys. Rev. **73**, 679, (1947).

[12] A. G. Redfield, Phys. Rev. **98**, 1787, (1955).

[13] R. Kubo and K. Tomita, J. Phys. Soc. Japan. **9**, 888, (1954).

[14] A. Abragam, *Principles of Nuclear Magnetism* (Oxford, New York, 2006), Chap. 3.

[15] C. P. Slichter, *Principles of Magnetic Resonance* (Springer, Berlin, 1990), Chap. 6.

[16] P. T. Callaghan, *Translational Dynamics & Magnetic Resonance: Principles of Pulsed Gradient Spin Echo NMR* (Oxford, New York, 2011), Chap. 4.

[17] A. J. Shaka, J. Keeler, T. Frenkiel and R. Freeman, J. Magn. Reson. **52**, 335, (1983).

[18] K. D. Pavuluri and K. V. Ramanathan, Magn. Reson. Chem. **54**, 151, (2016).

[19] P. Mansfield, J. Phys. E: Sci. Instrum. **21**, 18, (1988).

[20] E. Fukushima and S. B. W. Roeder, *Experimental Pulse NMR: A Nuts and Bolts Approach* (Westview Press, USA, 1981), Chap. 3.

[21] H. Y. Carr and E. M. Purcell, Phys. Rev. **94**, 630, (1954).

[22] S. Meiboom, D. Gill, Rev. Sci. Instrum. **29**, 688, (1958). 21

[23] D. Samios and T. Dorfmüller, Chem. Phys. Lett. **112**, 165, (1985). 22

[24] K. Tanabe, Chem. Phys. **31**, 319, (1978). 23

[25] K. T. Gillen and J. E. Griffiths, Chem. Phys. Lett. **17**, 359, (1972). 24

[26] N. R. Jber, A. A. Rashad, M. S. Shihab, J. Mol. Struct. **1043**, 28, (2013) [Supplementary material]. 25

[27] N. Weiner, *The Fourier Integral and Certain of Its Applications* (Cambridge, London, 1933), Chap. 1.